Chirality-matched catalyst-controlled macrocyclization reactions

Jaeyeon Hwang[a], Brandon Q. Mercado[a], and Scott J. Miller[a,1]

[a]Department of Chemistry, Yale University, New Haven, CT 06520

This contribution is part of the special series of Inaugural Articles by members of the National Academy of Sciences elected in 2020.

Contributed by Scott J. Miller, July 16, 2021 (sent for review July 16, 2021; reviewed by Phil S. Baran and David W. C. MacMillan)

Macrocycles, formally defined as compounds that contain a ring with 12 or more atoms, continue to attract great interest due to their important applications in physical, pharmacological, and environmental sciences. In syntheses of macrocyclic compounds, promoting intramolecular over intermolecular reactions in the ring-closing step is often a key challenge. Furthermore, syntheses of macrocycles with stereogenic elements confer an additional challenge, while access to such macrocycles are of great interest. Herein, we report the remarkable effect peptide-based catalysts can have in promoting efficient macrocyclization reactions. We show that the chirality of the catalyst is essential for promoting favorable, matched transition-state relationships that favor macrocyclization of substrates with preexisting stereogenic elements; curiously, the chirality of the catalyst is essential for successful reactions, even though no new static (i.e., not "dynamic") stereogenic elements are created. Control experiments involving either achiral variants of the catalyst or the enantiomeric form of the catalyst fail to deliver the macrocycles in significant quantity in head-to-head comparisons. The generality of the phenomenon, demonstrated here with a number of substrates, stimulates analogies to enzymatic catalysts that produce naturally occurring macrocycles, presumably through related, catalyst-defined peripheral interactions with their acyclic substrates.

macrocyclization | asymmetric catalysis | peptides | cross-coupling | stereochemistry

Macrocyclic compounds are known to perform a myriad of functions in the physical and biological sciences. From cyclodextrins that mediate analyte separations (1) to porphyrin cofactors that sit in enzyme active sites (2, 3) and to potent biologically active, macrocyclic natural products (4) and synthetic variants (5–7), these structures underpin a wide variety of molecular functions (Fig. 1*A*). In drug development, such compounds are highly coveted, as their conformationally restricted structures can lead to higher affinity for the desired target and often confer additional metabolic stability (8–13). Accordingly, there exists an entire synthetic chemistry enterprise focused on efficient formation and functionalization of macrocycles (14–18).

In syntheses of macrocyclic compounds, the ring-closing step is often considered the most challenging step, as competing di- and oligomerization pathways must be overcome to favor the intramolecular reaction (14). High-dilution conditions are commonly employed to favor macrocyclization of linear precursors (19). Substrate preorganization can also play a key role in overcoming otherwise high entropic barriers associated with multiple conformational states that are not suited for ring formation. Such preorganization is most often achieved in synthetic chemistry through substrate design (14, 20–22). Catalyst or reagent controls that impose conformational benefits that favor ring formation are less well known. Yet, critical precedents include templating through metal-substrate complexation (23, 24), catalysis by foldamers (25) or enzymes (26–29), or, in rare instances, by small molecules (discussed below). Characterization of biosynthetic macrocyclization also points to related mechanistic issues and attributes for efficient macrocyclizations (30–34). Coupling macrocyclization reactions to the creation of stereogenic elements is also rare (35). Metal-mediated reactions have been applied toward stereoselective macrocyclizations wherein chiral ligands transmit stereochemical information to the products (Fig. 1*B*). For example, atroposelective ring closure via Heck coupling has been applied in the asymmetric total synthesis of isoplagiochin D by Speicher and coworkers (36–40). Similarly, atroposelective syntheses of (+)-galeon and other diarylether heptanoid natural products were achieved via Ullman coupling using *N*-methyl proline by Salih and Beaudry (41). Finally, Reddy and Corey reported the enantioselective syntheses of cyclic terpenes by In-catalyzed allylation utilizing a chiral prolinol-based ligand (42). While these examples collectively illustrate the utility of chiral ligands in stereoselective macrocyclizations, such examples remain limited.

We envisioned a different role for chiral catalysts when addressing intrinsically disfavored macrocyclization reactions. When unfavorable macrocyclization reactions are confronted, we hypothesized that a catalyst–substrate interaction might provide transient conformational restriction that could promote macrocyclization. To address this question, we chose to explore whether or not a chiral catalyst-controlled macrocyclization might be possible with peptidyl copper complexes. In the context of

Significance

Chiral catalysts are generally used to control stereochemistry in organic reactions. Generally, they control enantioselectivity or diastereoselectivity. In recent years, applications have expanded to include control over site selectivity in reactions involving complex molecules. Even more rarely, they can control chemoselectivity along with stereochemistry. We report herein that a carefully chosen chiral catalyst can also be decisive for efficient macrocyclization reactions in cases where simple achiral catalysts or stereochemically mismatched catalysts fail. Notably, in these reactions, a chiral catalyst proves essential for control of a reaction in which no new static (i.e., not "dynamic") stereogenic elements are introduced. While fundamentally intriguing, these observations could also influence strategies for efficient synthesis of macrocyclic compounds in a variety of settings.

Author contributions: J.H. and S.J.M. designed research; J.H. and B.Q.M. performed research; J.H., B.Q.M., and S.J.M. analyzed data; and J.H., B.Q.M., and S.J.M. wrote the paper.

Reviewers: P.S.B., The Scripps Research Institute; and D.W.C.M., Princeton University.

The authors declare no competing interest.

Published under the PNAS license.

[1]To whom correspondence may be addressed. Email: scott.miller@yale.edu.

This article contains supporting information online at https://www.pnas.org/lookup/suppl/doi:10.1073/pnas.2113122118/-/DCSupplemental.

Published October 1, 2021.

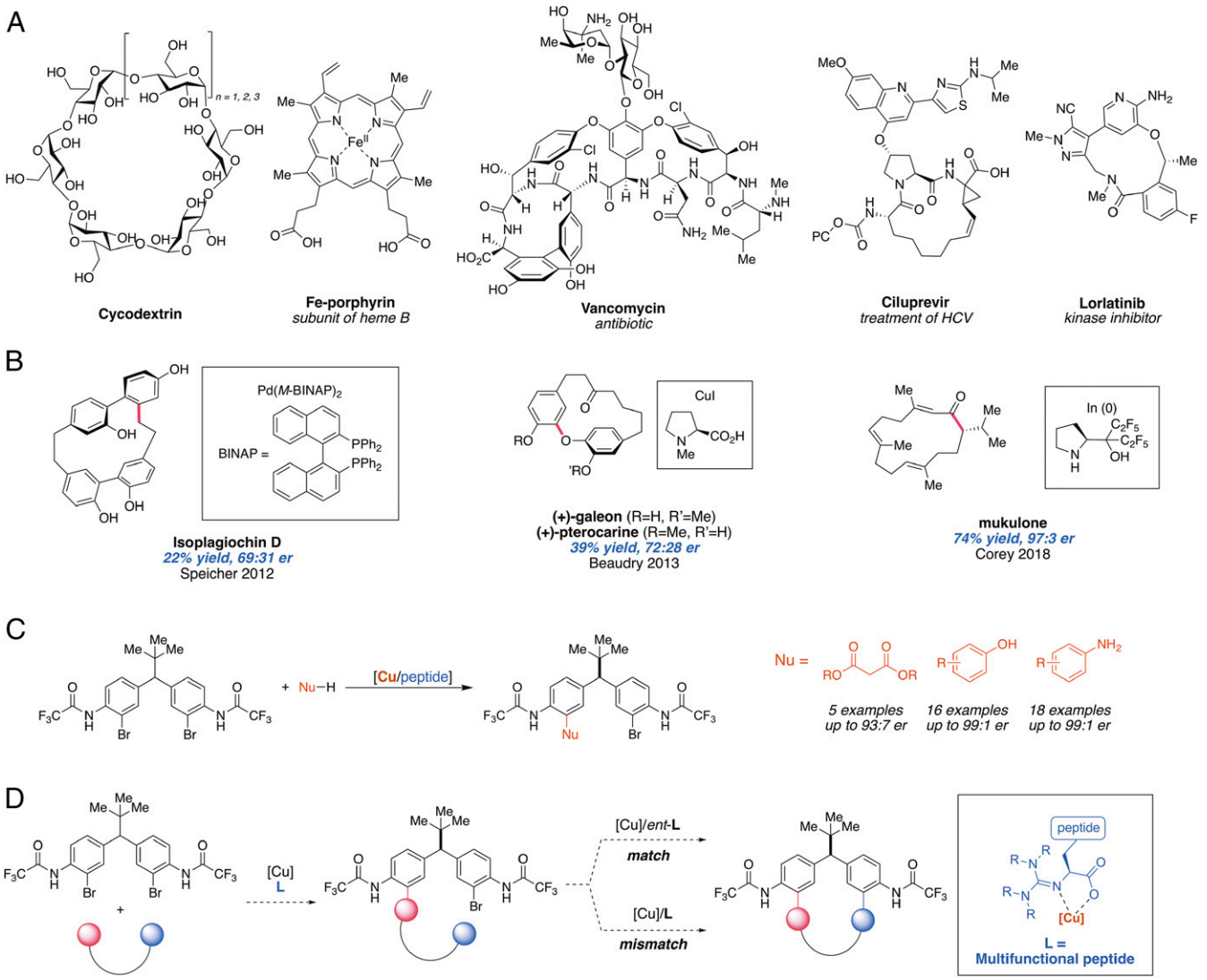

Fig. 1. (*A*) Examples of macrocyclic compounds with important applications. HCV, hepatitis C virus. (*B*) Use of chiral ligands in metal-catalyzed or mediated stereoselective macrocyclization reactions. (*C*) Remote desymmetrization using guanidinylated ligands via Ullmann coupling. (*D*) This work: use of copper/peptidyl complexes for macrocyclization and the exploration of matched and mismatched effect.

the medicinally ubiquitous diarylmethane scaffold, we had previously demonstrated the capacity for remote asymmetric induction in a series of bimolecular desymmetrizations using bifunctional, tetramethylguanidinylated peptide ligands. For example, we showed that peptidyl copper complexes were able to differentiate between the two aryl bromides during C–C, C–O, and C–N cross-coupling reactions (Fig. 1*C*) (43–45). Moreover, in these intermolecular desymmetrizations, a correlation between enantioselectivity and conversion was observed, revealing the catalyst's ability to perform not only enantiotopic group discrimination but also kinetic resolution on the monocoupled product as the reaction proceeds (44). This latter observation stimulated our speculation that if an internal nucleophile were present to undergo intramolecular cross-coupling to form a macrocycle, stereochemically sensitive interactions (so-called matched and mismatched effects) (46) could be observed (Fig. 1*D*). Ideally, we anticipated that transition state–stabilizing interactions might even prove decisive in matched cases, and the absence of catalyst–substrate stabilizing interactions might account for the absence of macrocyclization for these otherwise intrinsically unfavorable reactions. Herein, we disclose the explicit observation of these effects in chiral catalyst-controlled macrocyclization reactions.

Results and Discussion

Our investigation began with design of a suitable bifunctional nucleophile. A critical issue involves site selectivity. That is, we envisioned a sequential desymmetrization–macrocyclization, wherein one reaction partner would bear two electrophilic aryl halide sites (Fig. 2, **1**), while the coupling partner would contain two different nucleophilic sites (Fig. 2, **2a**). The order of reactivity on the two nucleophilic sites of **2a** was established through a series of competition experiments (see *SI Appendix*, section 7.1). For example, we found that a chemoselective coupling of diethyl malonate to **1** occurs in the presence of an unprotected aniline. In agreement with these competition experiments, **2a** underwent chemo- and enantioselective C–C coupling using **L1** to give **3a** under Ullmann coupling conditions (66% yield, 94:6 er) (43). Then, using ligand *ent*-**L2** (enantiomeric at each stereogenic center with respect to **L1**), macrocycle **4a** was obtained in 67% yield, and with further enantioenrichment to >99:1 er (Fig. 2, Eq. **2**; see *SI Appendix*, section 9 for

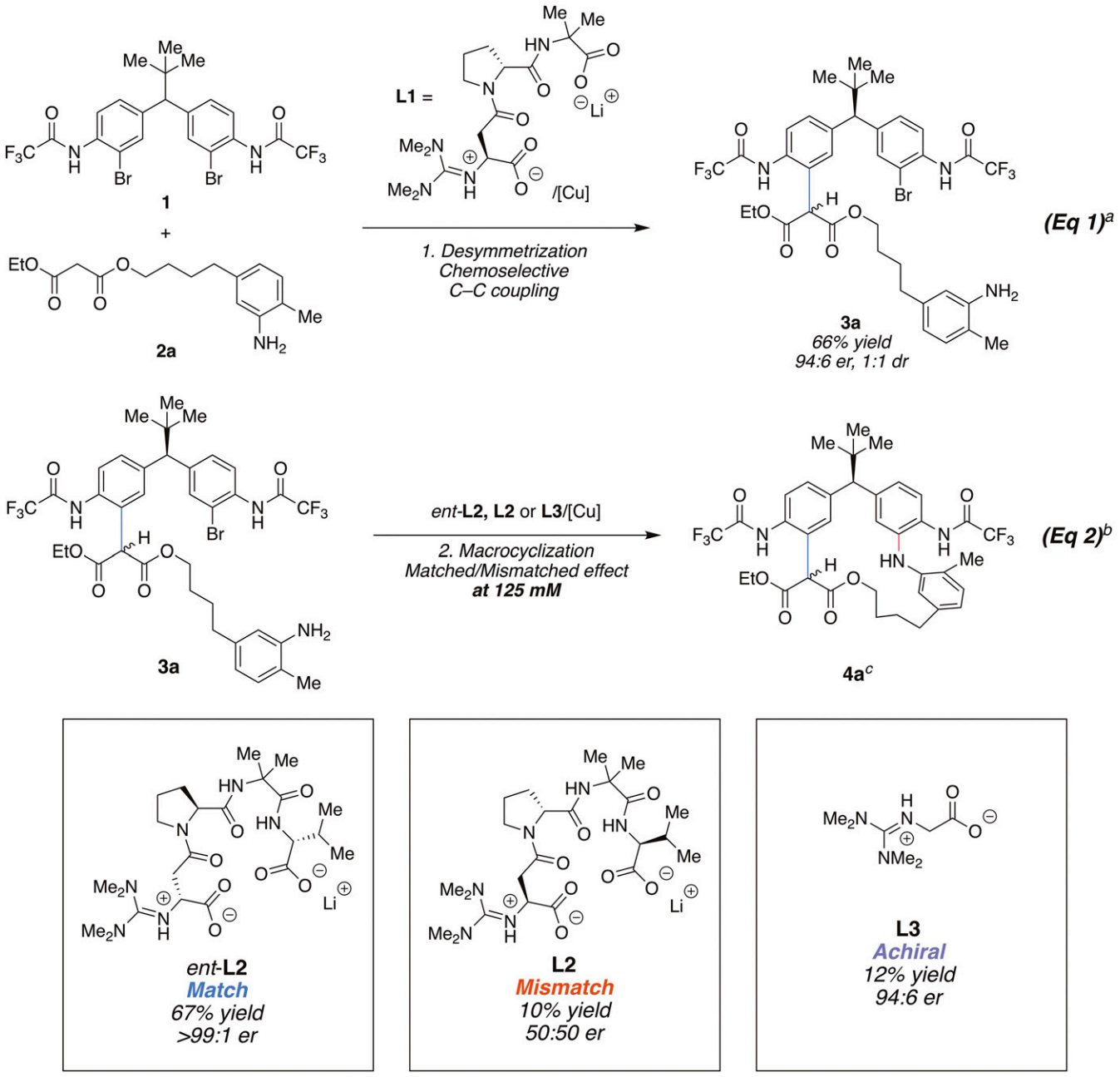

Fig. 2. Chemo- and enantioselectiselective C–C coupling followed by diastereodifferentiating macrocyclization by C–N coupling. [a]Reaction conditions 1: **1** (1.8 mmol, 1.0 equiv), **2a** (1.0 equiv), $Cu(MeCN)_4BF_4$ (5 mol %), **L1** (10 mol %), Cs_2CO_3 (4.2 equiv), 1:2 DMF/toluene (0.25 M), room temperature, 15 h. [b]Reaction conditions 2: **3a** (0.15 mmol, 1.0 equiv), CuBr (20 mol %), ligand (40 mol %), K_3PO_4 (4.4 equiv), 1:2 DMF/MeCN (0.125 M), 45 °C, 15 h. [c]1.8:1 dr (diastereomeric ratio) in CD_2Cl_2. dr of **4a** varies in different solvents and concentrations.

optimization). As is typical with α-substituted malonates, this product is isolated as a mixture of epimerizable diastereomers due to the lability of the malonate stereogenic center. The choice of *ent*-**L2** as the ligand for the macrocyclization catalyst was born of its discovery as an excellent ligand for enantioselective C–N bond-forming cross-couplings (45). In contrast, use of **L2** (the enantiomer of the successfully employed *ent*-**L2**) failed to deliver the macrocycle in good yield, delivering **4a** in only 10% yield, and in racemic form. In fact, what macrocyclization is observed using the mismatched ligand **L2** appears to be the result of the processing of the residual minor enantiomer (which is matched to **L2**), as evidenced by the recovery of enantiopure, unreacted starting material **3a** after the macrocyclization (see *SI Appendix*, section 8.5; see also *SI Appendix*, Section 11, which also supports this assertion of kinetic resolution). Furthermore, in a striking control experiment, the achiral guanidinylated ligand **L3** also performed poorly and quite similarly to the mismatched **L2**. These results highlight the critical nature of the stereochemically matched ligand for successful cyclization and also point strongly to stabilizing cooperative effects between the right chiral catalyst and its matched substrate during the macrocyclization step. Notably, in the matched case, the macrocyclization proceeds at 45 °C and under surprisingly typical concentrations for

https://doi.org/10.1073/pnas.2113122118

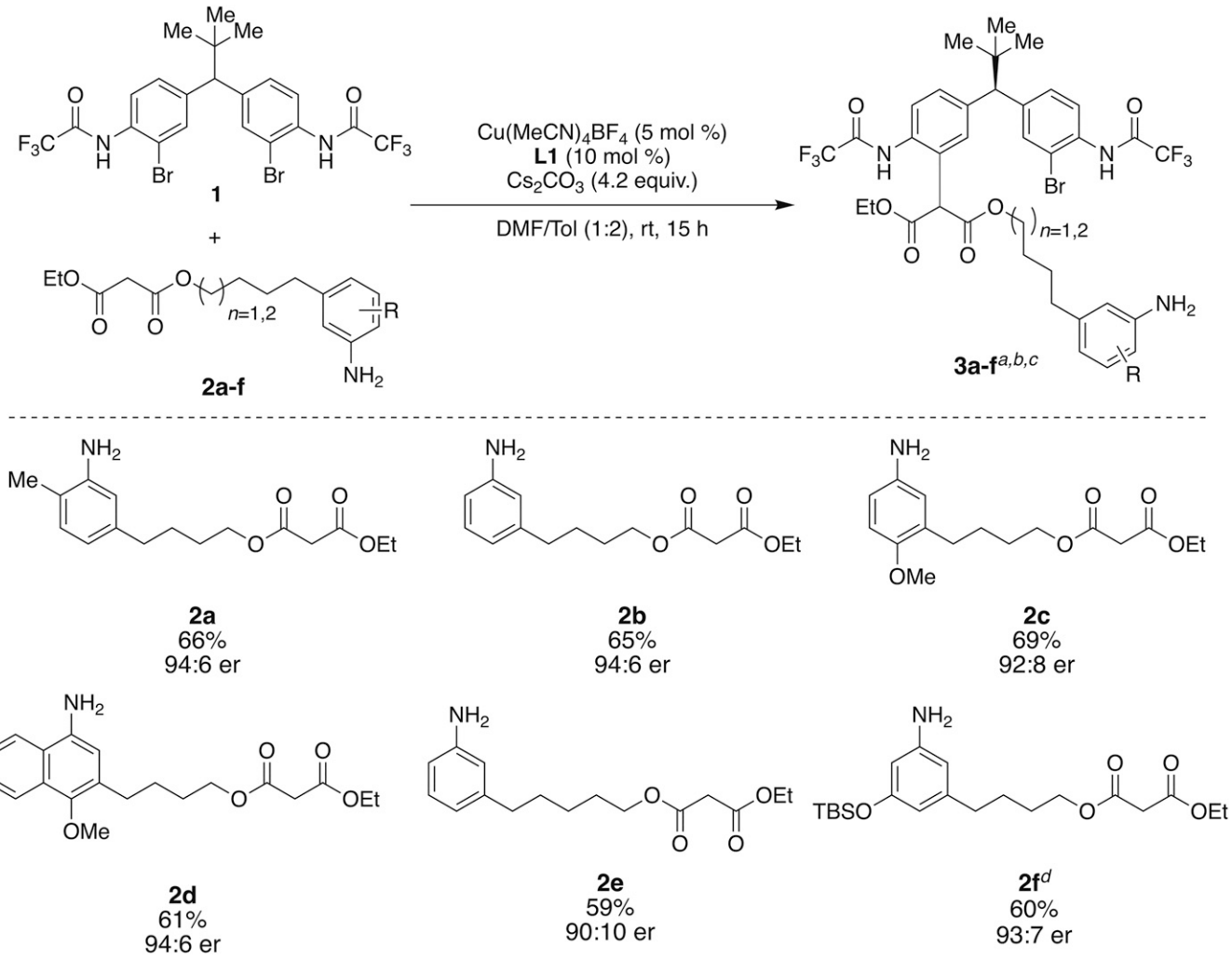

Fig. 3. Preparation of linear precursors by chemo- and enantioselective C–C coupling. [a]Isolated yields. [b]Enantiomeric ratios were determined using chiral HPLC analysis. [c]Products **3a** to **3f** are isolated in 1:1 dr (diastereomeric ratio). [d]In preparation of **3f**, TBS group was removed after C–C coupling step. See *SI Appendix*, section 8.3 for details. rt, room temperature; Tol, toluene.

many bimolecular reactions (125 mM); extreme dilution, as is typical for many macrocyclizations (~1 mM), was not required (14–19).

Encouraged by the above results, linear precursors **3a** to **3f** were prepared to explore the scope of the reaction (Fig. 3; see *SI Appendix*, sections 4 and 6 for synthesis of **2a** to **2f**). As with **2a**, each substrate underwent chemo- and enantioselective C–C coupling to yield **3a** to **3f** in 59 to 69% yield, and with enantioselectivities ranging from 94:6 er to 90:10 er (Fig. 3), setting the stage for evaluation of the generality of the chirality-matched catalyst-controlled macrocyclizations.

In each case the special significance of the stereochemically matched ligand was evident. Moreover, in these successful macrocyclizations further enantioenrichment was observed in the products, while the mismatched and achiral ligands consistently gave poor results (Fig. 4*A*). For example, as illustrated in Fig. 2, macrocyclization of **3a** leads to the formation of 18-membered ring (**4a**) in 67% yield in excellent er (>99:1 er) using *ent*-**L2** (Fig. 4*A*). An *ortho* substituent is not necessary for the demonstration of ligand effect as seen in **3b** (50% yield, >99:1 er). However, the presence of an *ortho* substituent appears to aid in improving the yield of macrocyclized products, possibly by favoring intramolecular reaction over oligomerization pathways (**3a** and **3c**; see *SI Appendix*, section 13). The effect of the mismatched ligand was less apparent for **3d**, which appeared to be inherently more reactive—nevertheless, the matched ligand still dramatically outperformed the mismatched or the achiral ligands for this substrate. Linear precursor containing five methylene linkers (**3e**) also underwent macrocyclization. In this case, a 10-fold difference in the yield of macrocyclized product (**4e**) was observed, as *ent*-**L2** afforded the product in 23% yield (98:2 er), while **L2** leads to formation of the product in only 2.5% yield (32:68 er), which once again clearly demonstrates the importance of the matched ligand in the macrocyclization. Strikingly, a free phenol in the substrate is tolerated, as **3f** is processed to **4f** in 43% yield and with 99:1 er via the preferential intramolecular C–N coupling of **3f** using *ent*-**L2**(C–N, **4f**/C–O, **5f** = 7.2:1; Fig. 4*B*).

A particularly interesting observation is that the use of achiral ligand **L3** actually favored macrocyclization via C–O coupling (**5f**, 11% yield) and only gave the desired C–N linked macrocycle **4f** in 3% yield. We then explored whether we can overturn the observed selectivity by using a different guanidinylated ligand. Unfortunately, the use of a ligand previously optimized for C–O coupling, **L4** (44), did not lead to efficient macrocyclization, through either C–O coupling or C–N coupling, and only favored

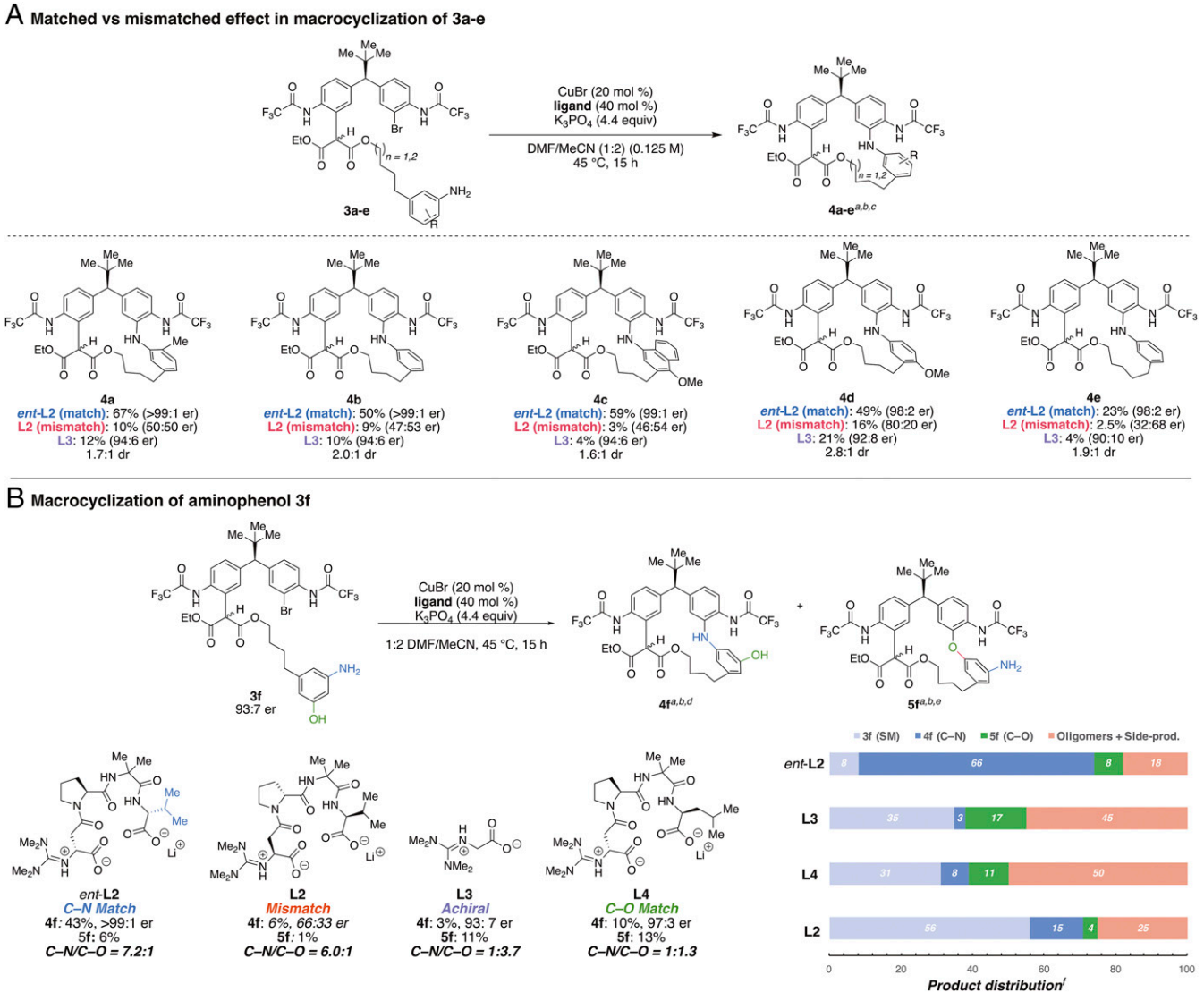

Fig. 4. (*A*) Macrocyclization of **3a** to **3e**: matched and mismatched effect. [a]Isolated yields. [b]Enantiomeric ratios were determined using chiral high-performance liquid chromatography analysis. [c]Diastereomeric ratio (dr) was determined by ^{1}H NMR in CD_2Cl_2. (*B*) Macrocyclization of aminophenol **3f** using different ligands. [d]**4f** is observed as a 2.5:1 mixture of diastereomers at 25 °C in CD_2Cl_2 by ^{1}H NMR. [e]**5f** is observed as a 4.3:1 mixture of diastereomers. [f]Product distribution based on uncorrected peak integration on ultraperformance liquid chromatography–mass spectrometry (UPLC-MS) peaks. See *SI Appendix*, section 14 for UPLC-MS traces.

intramolecular C–O coupling by a slight margin (1:1.3 ratio). Consistent with previous examples (Fig. 4*A*), the use of mismatched ligand **L2** is far less efficient in catalyzing macrocyclization. We speculate that in each case of an unfavorable reaction, oligomerized side products appear at the heart of inefficiency.

We then turned our attention to structural features of these new macrocycles. Notably, these large rings exhibit stereodynamic properties. Two sets of peaks are observed by ^{1}H NMR spectroscopy, with the ratio of two apparent diastereomers, (*S*, *S*)-**4a** and (*S*, *R*)-**4a**, varying as a function of different NMR solvents (see *SI Appendix*, section 15.3). While various phenomena might account for this observation (atropisomerism and conformational isomerism) (41, 47–54), we speculated instead that this phenomenon is due to slow epimerization of the malonate stereocenter via keto-enol tautomerization. Indeed, a complete deuterium exchange in methanol-d_4 is observed but requires 2 h to reach completion (Fig. 5). The connectivity and the absolute stereochemistry of these macrocycles were unambiguously determined by X-ray crystallography (Fig. 6*A*).

Finally, the basis of the observed stereochemical matched and mismatched effect in macrocyclization remains of interest. We posit that the following scenario enables chirality matched macrocyclization with peptidyl complexes (Fig. 6*B*). First, C–C coupling occurs on one aryl bromide of diarylmethane **1** using **L1** to afford the linear precursor **3a**. Then, the matched ligand (*ent*-**L2**), which is enantiomeric at the *i* (Asp residue) and the *i+1* (Pro residue) positions compared to **L1**, is able to efficiently catalyze macrocyclization by localizing the copper in close proximity to the aryl ring that bears the second substituting bromide (*Int-2*). On the other hand, the use of the mismatched ligand, **L2**, leads to a sluggish reaction, as its intrinsic chirality preference is to localize the copper center in proximity to the ring that already underwent C–C coupling, and which therefore no longer bears a bromide atom (*Int-3*).

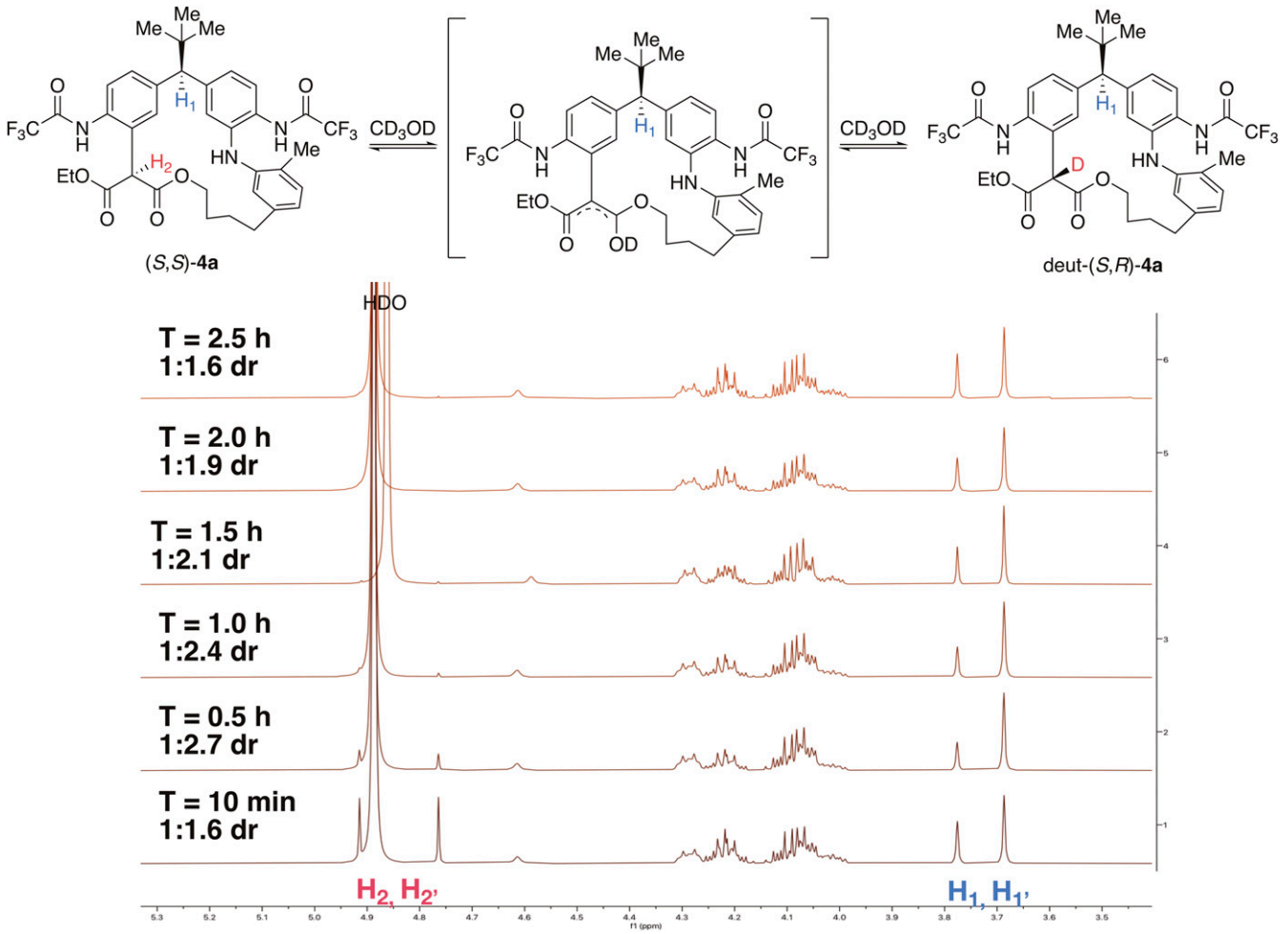

Fig. 5. Deuterium incorporation of **4a** in methanol-d_4. dr, diastereomeric ratio.

Presumably, the stereogenic centers of the matched catalyst are ultimately responsible for the low-energy conformations associated with the facile macrocyclization transition state. In contrast, the mismatched ligand would then lead to a higher energy transition state that likely suffers from unfavorable, stereochemically dictated interactions. Finally, in case of the achiral ligand **L3**, the lack of additional interaction between the carboxylate "tail" of the peptide ligand and the aryl ring may be contributing to a lower efficiency in macrocyclization (*Int-4*).

Conclusions

Chiral catalysts are generally employed to mediate reactions that create permanent, or at least persistent, stereogenic elements. We have shown here that they can play a decisive role in macrocyclization reactions wherein no new nonequilibrating element of chirality is actually formed; that is, stereochemical issues exist in transition states emanating from substrates with preexisting chirality and prove decisive for bond formation. Pragmatically, chiral catalysts can thus promote macrocyclization reactions that might otherwise not occur, or that might only occur under conditions of extremely high dilution. Fundamentally, the reported observations reveal a capacity of chiral catalysts to allow highly unfavorable ring formations through management of otherwise unfavorable entropy. While these observations are now recorded in venerable scaffold of interest to medicinal chemists, future work will explore the generality of this phenomenon.

Materials and Methods

General Procedure for Macrocyclization by C–N Coupling. K_3PO_4 (0.1401 g, 0.66 mmol, 4.40 equiv) was flamed-dried under vacuum in a 5-mL Schlenk flask. Upon cooling to room temperature, CuBr (0.0043 g, 0.03 mmol, 0.20 equiv), peptide ligand (0.06 mmol, 0.40 equiv), and a magnetic stir bar were added to the flask. The flask was sealed with a new rubber septum and further secured with Parafilm. The flask was evacuated for 5 min and backfilled with N_2. This process was repeated two additional times. A 1:2 *N*,*N*-dimethylformamide (DMF)/MeCN mixture (0.8 mL) was added through the septum, and the mixture was allowed to stir for 15 min at room temperature, after which diarylmethane **3a** to **3f** (0.15 mmol, 1.00 equiv) in MeCN (0.2 mL) was added. The vial was rinsed with DMF (0.2 mL), which was also added to the reaction mixture. The reaction mixture was left to stir for 15 h at 45 °C. After 15 h, the reaction mixture was diluted with EtOAc (10 mL) and transferred to a separatory funnel. The organic layer was washed with saturated NH_4Cl (aq) (10 mL). The organic layer was separated and the aqueous layer was extracted with EtOAc (5 mL, three times). Combined organic layers were washed with sat. NaCl (aq) (30 mL), dried over Na_2SO_4, filtered, and concentrated *in vacuo*. The product was purified by flash chromatography with EtOAc/Hex gradient.

Data Availability. All study data are included in the article and *SI Appendix*.

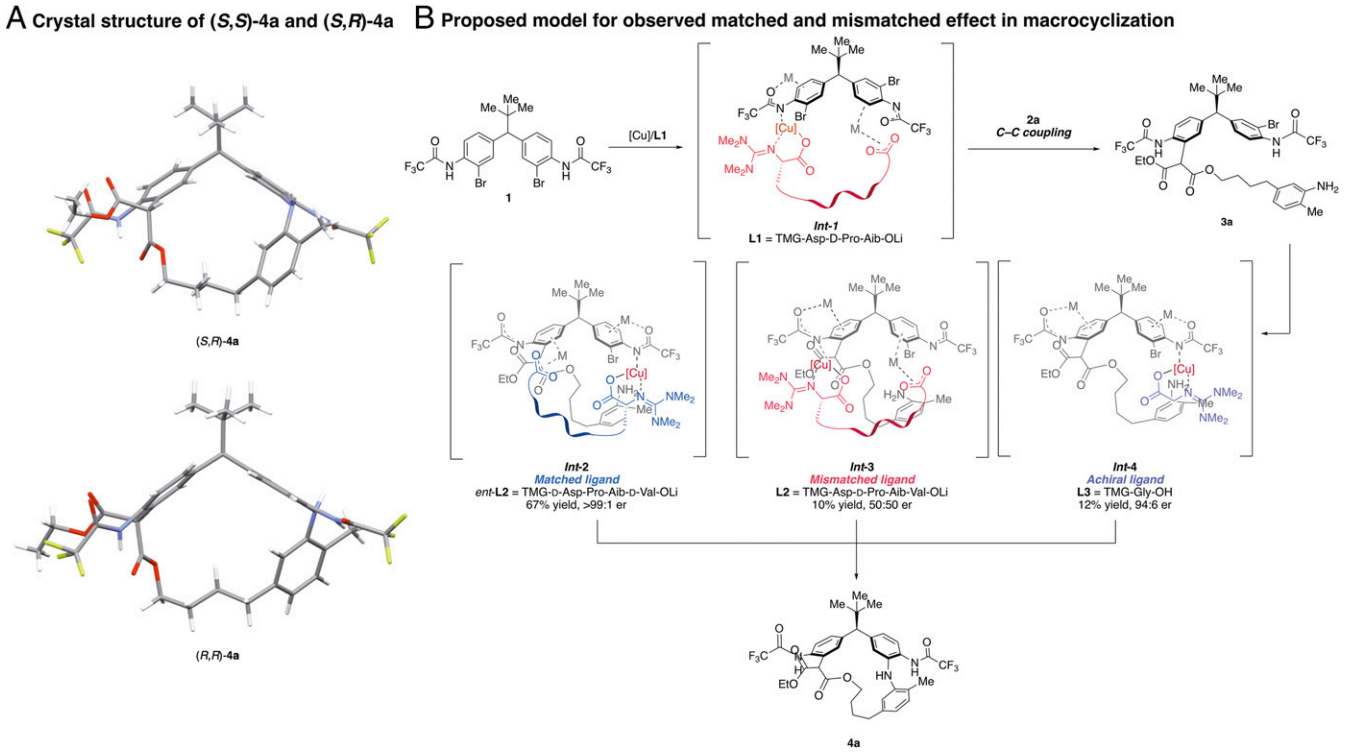

Fig. 6. (*A*) Crystal structures of (*S, S*)-**4a** and (*S, R*)-**4a**, revealing the presence of both malonate epimers in a unit cell. (*B*) Proposed model for stereochemical matched and mismatched effect in macrocyclization of diarylmethanes.

ACKNOWLEDGMENTS. This work was supported by the National Institute of General Medical Sciences (NIH grant R35 GM132092 to S.J.M.). We thank Dr. Alex J. Chinn, Dr. Byoungmoo Kim, and Dr. Yongseok Kwon for their advice and materials. We also thank Dr. Eric Paulson for assistance with NMR spectroscopy and Dr. Fabian Menges for assistance with mass spectrometry.

1. L. Szente, J. Szemán, Cyclodextrins in analytical chemistry: Host-guest type molecular recognition. *Anal. Chem.* **85**, 8024–8030 (2013).
2. W. S. Caughey, Porphyrin proteins and enzymes. *Annu. Rev. Biochem.* **36**, 611–644 (1967).
3. K. M. Smith, "Porphyrins" in *Comprehensive Coordination Chemistry II*, J. A. McCleverty, T. J. Meyer, Eds. (Pergamon, Oxford, 2003), vol. 2, pp. 493–506.
4. D. J. Newman, G. M. Cragg, "Bioactive macrocycles from nature" in *Macrocycles in Drug Discovery*, J. I. Levin, Ed. (The Royal Society of Chemistry, 2015), pp. 1–36.
5. S. Vendeville, M. D. Cummings, "Synthetic macrocycles in small-molecule drug discovery" in *Annual Reports in Medicinal Chemistry*, M. C. Desai, Ed. (Academic Press, 2013), vol. 48, pp. 371–386.
6. E. Marsault, M. L. Peterson, Macrocycles are great cycles: Applications, opportunities, and challenges of synthetic macrocycles in drug discovery. *J. Med. Chem.* **54**, 1961–2004 (2011).
7. J. A. Amrhein, S. Knapp, T. Hanke, Synthetic opportunities and challenges for macrocyclic kinase inhibitors. *J. Med. Chem.* **64**, 7991–8009 (2021).
8. E. M. Driggers, S. P. Hale, J. Lee, N. K. Terrett, The exploration of macrocycles for drug discovery—An underexploited structural class. *Nat. Rev. Drug Discov.* **7**, 608–624 (2008).
9. F. Giordanetto, J. Kihlberg, Macrocyclic drugs and clinical candidates: What can medicinal chemists learn from their properties? *J. Med. Chem.* **57**, 278–295 (2014).
10. E. A. Villar *et al.*, How proteins bind macrocycles. *Nat. Chem. Biol.* **10**, 723–731 (2014).
11. A. A. Vinogradov, Y. Yin, H. Suga, Macrocyclic peptides as drug candidates: Recent progress and remaining challenges. *J. Am. Chem. Soc.* **141**, 4167–4181 (2019).
12. J. Mallinson, I. Collins, Macrocycles in new drug discovery. *Future Med. Chem.* **4**, 1409–1438 (2012).
13. X. Li, S. Chen, W.-D. Zhang, H.-G. Hu, Stapled helical peptides bearing different anchoring residues. *Chem. Rev.* **120**, 10079–10144 (2020).
14. V. Martí-Centelles, M. D. Pandey, M. I. Burguete, S. V. Luis, Macrocyclization reactions: The importance of conformational, configurational, and template-induced preorganization. *Chem. Rev.* **115**, 8736–8834 (2015).
15. I. Saridakis, D. Kaiser, N. Maulide, Unconventional macrocyclizations in natural product synthesis. *ACS Cent. Sci.* **6**, 1869–1889 (2020).
16. A. Fürstner, Lessons from natural product total synthesis: Macrocyclization and postcyclization strategies. *Acc. Chem. Res.* **54**, 861–874 (2021).
17. H. Itoh, M. Inoue, Comprehensive structure-activity relationship studies of macrocyclic natural products enabled by their total syntheses. *Chem. Rev.* **119**, 10002–10031 (2019).
18. C. J. White, A. K. Yudin, Contemporary strategies for peptide macrocyclization. *Nat. Chem.* **3**, 509–524 (2011).
19. L. Rossa, F. Vögtle, "Synthesis of medio- and macrocyclic compounds by high dilution principle techniques" in *Cyclophanes I. Topics in Current Chemistry*, F. Vögtle, Ed. (Springer, Berlin, 1983), vol. 113, pp. 3–76.
20. S. J. Miller, H. E. Blackwell, R. H. Grubbs, Application of ring-closing metathesis to the synthesis of rigidified amino acids and peptides. *J. Am. Chem. Soc.* **118**, 9606–9614 (1996).
21. J. Blankenstein, J. Zhu, Conformation-directed macrocyclization reactions. *Eur. J. Org. Chem.* **2005**, 1949–1964 (2005).
22. V. Adebomi *et al.*, CyClick chemistry for the synthesis of cyclic peptides. *Angew. Chem. Int. Ed. Engl.* **58**, 19073–19080 (2019).
23. C. S. Higman *et al.*, Chelate-assisted ring-closing metathesis: A strategy for accelerating macrocyclization at ambient temperatures. *J. Am. Chem. Soc.* **140**, 1604–1607 (2018).
24. M. Yu *et al.*, Synthesis of macrocyclic natural products by catalyst-controlled stereoselective ring-closing metathesis. *Nature* **479**, 88–93 (2011).
25. Z. C. Girvin, M. K. Andrews, X. Liu, S. H. Gellman, Foldamer-templated catalysis of macrocycle formation. *Science* **366**, 1528–1531 (2019).
26. C. M. Czekster, H. Ludewig, S. A. McMahon, J. H. Naismith, Characterization of a dual function macrocyclase enables design and use of efficient macrocyclization substrates. *Nat. Commun.* **8**, 1045–1055 (2017).
27. C. Zhang, P. Dai, A. M. Spokoyny, B. L. Pentelute, Enzyme-catalyzed macrocyclization of long unprotected peptides. *Org. Lett.* **16**, 3652–3655 (2014).
28. C. Ongpipattanakul, S. K. Nair, Biosynthetic proteases that catalyze the macrocyclization of ribosomally synthesized linear peptides. *Biochemistry* **57**, 3201–3209 (2018).
29. C. Gagnon *et al.*, Biocatalytic synthesis of planar chiral macrocycles. *Science* **367**, 917–921 (2020).
30. A. Caruso, R. J. Martinie, L. B. Bushin, M. R. Seyedsayamdost, Macrocyclization via an arginine-tyrosine crosslink broadens the reaction scope of radical *S*-adenosylmethionine enzymes. *J. Am. Chem. Soc.* **141**, 16610–16614 (2019).
31. S. C. Bobeica, L. Zhu, J. Z. Acedo, W. Tang, W. A. van der Donk, Structural determinants of macrocyclization in substrate-controlled lanthipeptide biosynthetic pathways. *Chem. Sci. (Camb.)* **11**, 12854–12870 (2020).
32. H. Nakamura, E. E. Schultz, E. P. Balskus, A new strategy for aromatic ring alkylation in cylindrocyclophane biosynthesis. *Nat. Chem. Biol.* **13**, 916–921 (2017).

33. H. L. Tran *et al*., Structure-activity relationship and molecular mechanics reveal the importance of ring entropy in the biosynthesis and activity of a natural product. *J. Am. Chem. Soc.* **139**, 2541–2544 (2017).
34. A. A. Koch *et al*., A single active site mutation in the pikromycin thioesterase generates a more effective macrocyclization catalyst. *J. Am. Chem. Soc.* **139**, 13456–13465 (2017).
35. K. Zheng, R. Hong, Stereoconfining macrocyclizations in the total synthesis of natural products. *Nat. Prod. Rep.* **36**, 1546–1575 (2019).
36. M. Groh, D. Meidlinger, G. Bringmann, A. Speicher, Atroposelective Heck macrocyclization: Enantioselective synthesis of bis(bibenzylic) natural products. *Org. Lett.* **14**, 4548–4551 (2012).
37. H. Uchiro *et al*., Total synthesis of Hirsutellone B via Ullmann-type direct 13-membered macrocyclization. *Org. Lett.* **13**, 6268–6271 (2011).
38. Q. Cai, G. He, D. Ma, Mild and nonracemizing conditions for Ullmann-type diaryl ether formation between aryl iodides and tyrosine derivatives. *J. Org. Chem.* **71**, 5268–5273 (2006).
39. D. L. Boger, M. A. Patane, J. Zhou, Total synthesis of bouvardin, O-Methylbouvardin, and O-Methyl-N9-desmethylbouvardin. *J. Am. Chem. Soc.* **116**, 8544–8556 (1994).
40. J. C. Collins, K. A. Farley, C. Limberakis, S. Liras, S. D. Price, K. James, Macrocyclizations for medicinal chemistry: Synthesis of druglike macrocycles by high-concentration Ullmann coupling. *J. Org. Chem.* **77**, 11079–11090 (2012).
41. M. Q. Salih, C. M. Beaudry, Enantioselective Ullmann ether couplings: Syntheses of (-)-myricatomentogenin, (-)-jugcathanin, (+)-galeon, and (+)-pterocarine. *Org. Lett.* **15**, 4540–4543 (2013).
42. D. S. Reddy, E. J. Corey, Enantioselective conversion of oligoprenol derivatives to macrocycles in the germacrene, cembrene, and 18-membered cyclic sesterterpene series. *J. Am. Chem. Soc.* **140**, 16909–16913 (2018).
43. B. Kim *et al*., Distal stereocontrol using guanidinylated peptides as multifunctional ligands: Desymmetrization of diarylmethanes via Ullman cross-coupling. *J. Am. Chem. Soc.* **138**, 7939–7945 (2016).
44. A. J. Chinn, B. Kim, Y. Kwon, S. J. Miller, Enantioselective intermolecular C-O bond formation in the desymmetrization of diarylmethines employing a guanidinylated peptide-based catalyst. *J. Am. Chem. Soc.* **139**, 18107–18114 (2017).
45. Y. Kwon, A. J. Chinn, B. Kim, S. J. Miller, Divergent control of point and axial stereogenicity: Catalytic enantioselective C-N bond-forming cross-coupling and catalyst-controlled atroposelective cyclodehydration. *Angew. Chem. Int. Ed. Engl.* **57**, 6251–6255 (2018).
46. S. Masamune, W. Choy, J. S. Petersen, L. R. Sita, Double asymmetric synthesis and a new strategy for stereochemical control in organic synthesis. *Angew. Chem. Int. Ed. Engl.* **24**, 1–30 (1985).
47. E. Kumarasamy, R. Raghunathan, M. P. Sibi, J. Sivaguru, Nonbiaryl and heterobiaryl atropisomers: Molecular templates with promise for atropselective chemical transformations. *Chem. Rev.* **115**, 11239–11300 (2015).
48. F. P. Gasparro, N. H. Kolodny, NMR determination of the rotational barrier in *N, N*-dimethylacetamide. A physical chemistry experiment. *J. Chem. Educ.* **54**, 258–261 (1977).
49. T. Eguchi *et al*., Unique solvent-dependent atropisomerism of a novel cytotoxic naphthoxanthene antibiotic FD-594. *J. Org. Chem.* **64**, 5371–5376 (1999).
50. S. B. Singh *et al*., The complestatins as HIV-1 integrase inhibitors. Efficient isolation, structure elucidation, and inhibitory activities of isocomplestatin, chloropeptin I, new complestatins, A and B, and acid-hydrolysis products of chloropeptin I. *J. Nat. Prod.* **64**, 874–882 (2001).
51. M. Schäfer, T. R. Schneider, G. M. Sheldrick, Crystal structure of vancomycin. *Structure* **4**, 1509–1515 (1996).
52. D. L. Boger *et al*., Thermal atropisomerism of teicoplanin aglycon derivatives: Preparation of the *P, P, P* and *M, P, P* atropisomers of the teicoplanin aglycon via selective equilibration of the DE ring system. *J. Am. Chem. Soc.* **122**, 10047–10055 (2000).
53. P. W. Glunz *et al*., Atropisomer control in macrocyclic factor VIIa inhibitors. *J. Med. Chem.* **59**, 4007–4018 (2016).
54. R. Costil, A. J. Sterling, F. Duarte, J. Clayden, Atropisomerism in diarylamines: Structural requirements and mechanisms of conformational interconversion. *Angew. Chem. Int. Ed. Engl.* **59**, 18670–18678 (2020).